LAWRENCE
LIVERMORE
NATIONAL
LABORATORY

LLNL-TR-660429

Atomic Interferometry with Detuned Counter-Propagating Electromagnetic Pulses

M. Y. Tsang

September 16, 2014

Disclaimer

This work performed under the auspices of the U.S. Department of Energy by Lawrence Livermore National Laboratory under Contract DE-AC52-07NA27344.

Atomic Interferometry with Detuned Counter-propagating Electromagnetic Pulses

Ming-Yee Tsang

5 September 2014

Abstract

Atomic fountain interferometry uses atoms cooled with optical molasses to 1 μK, which are then launched in a fountain mode. The interferometer relies on the nonlinear Raman interaction of counter-propagating visible light pulses. We present models of these key transitions through a series of Hamiltonians. Our models, which have been verified against special cases with known solutions, allow us to incorporate the effects of non-ideal pulse shapes and realistic laser frequency or wavevector jitter.

1 Motivation

The development of atomic interferometry in the early 1990s made possible an alternative method of highly sensitive gravity gradiometry. This sensitivity makes "gravity imaging" possible. By observing how atomic particles behave in the presence of even weak gravitational fields, one can predict how a gravitational source's mass is distributed.

One instrument for precisely measuring gravitational effects is the gravity gradiometer, which employs a pair of interferometers with common phase relations. These gradiometers employ atomic interferometry (a kind of double-path interferometry reminiscent of Mach-Zehnder interferometry) and are driven by counter-propogating laser beams, which act on atoms that travel in a vacuum pipe above a magneto-optical trap, causing energy-level transitions. Each laser beam is responsible for a different transition: one for the transition between the

ground state and an intermediate state and the other for the transition between the intermediate level and an excited state. Research on Raman transitions has enabled high-momentum transfer to atoms, which induces more substantial interferometric effects and therefore makes interference patterns easier to observe and measure.[1] Understanding these transitions and their consequences better will allow us to measure gravitation more accurately.

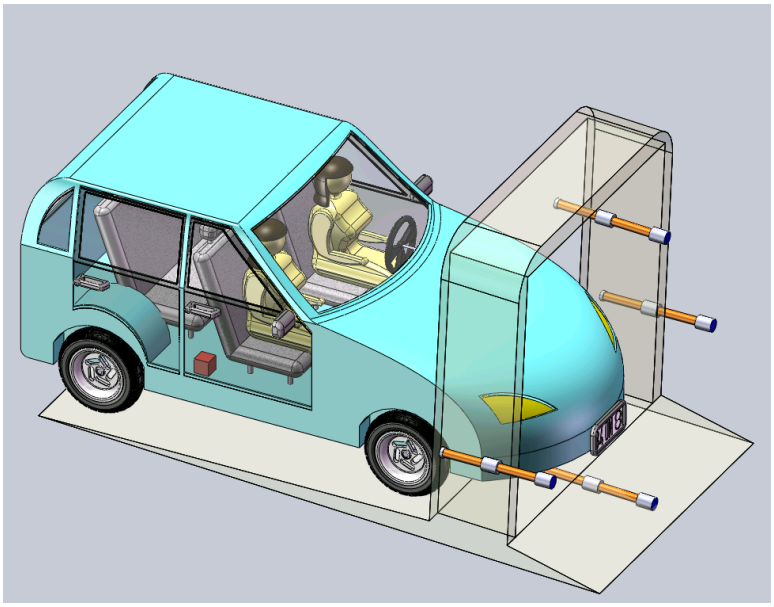

Figure 1

We are interested in detecting small excess masses (> 25 kg) in moving vehicles by differentiating their gravitational signatures from those of the vehicles (see Figure 1). Gravity gradiometers based on atomic-fountain interferometry are the most sensitive bias-drift-free sensors available. The key innovation enabling their high sensitivity is the use of Raman coupling to a high-$\vec{k}$ intermediate state, which makes interferometric effects more pronounced and therefore easier to measure.

2 The Problem

2.1 Microscopic understanding of basic interferometry

Cold atom interferometry exploits the fundamental wave-like nature of all particles. An important example of quantum mechanical interferometry is the atomic

double-slit experiment, which demonstrates the wave nature of atomic particles and the viability of exploiting this property in an interferometer.[2] For example, cæsium atoms at 1 μK have typical de Broglie wavelength of about .1 μm. This high degree of quantum coherence that this results in enables sensors that depend on quantum phase coherence.

2.2 Atomic interferometry

The key to atomic fountain interferometry is the three short laser pulses fired at the atoms after initial launch at approximately 3 m s^{-1}. By analogy with Mach-Zehnder interferometry, the $\frac{\pi}{2}$-pulses are like beam splitters, separating and combining the "paths", and the π-pulse acts like a mirror (see Figure 2). External masses then perturb the momentum of the atoms through their Earth-gravity-induced freefall trajectory. We measure the effect of that perturbation to infer the mass distribution. The key property behind its function is the coupling of

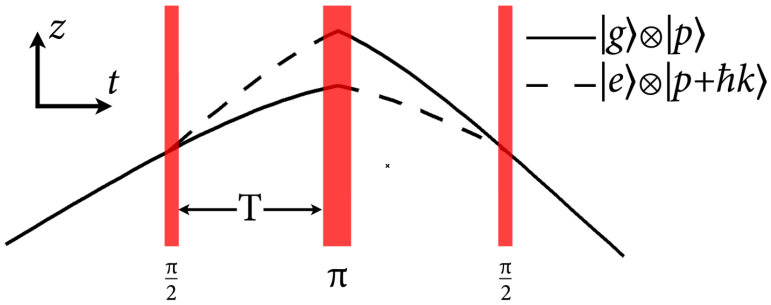

Figure 2

the atomic hyperfine states to the external momenta of the particles, allowing the overall wave function to be expressed as

$$|\phi(t)\rangle = \cos\left(\frac{\Omega t}{2}\right)|g, \vec{p}\rangle + e^{-i\frac{\pi}{2}} e^{i\phi_L} \sin\left(\frac{\Omega t}{2}\right)|e, \vec{p} + \hbar\vec{k}_{\text{eff}}\rangle,$$

where ϕ_L is the acquired phase from interaction with the electromagnetic pulse and the two kets are basis states formed by direct products between the hyperfine states and particle momentum that span the wave function Hilbert space.[3] For the $\frac{\pi}{2}$ and π pulses, $\Omega t = \frac{\pi}{2}$ and π, respectively. Interferometry is conceptually driven, of course, by a separation and recombination of waves and the subsequent measurement of their phases. In order to "separate" the particles' wavefunctions, one imparts an initial "kick" for the particles to take two different "paths". A

second kick reflects the paths, so that the particles begin to reconverge. A third kick "combines" the paths again, so that the two waves' phase difference may be measured. (This is analogous to Mach-Zehnder interferometry, in which the $\frac{\pi}{2}$-pulses are comparable to beam splitters and the π-pulse acts like a mirror.) The final measurement is of the resultant phase shift, which is essentially doppler shift, given by $\Delta\phi = \vec{k} \cdot \delta\vec{x}$.

2.3 The Raman transition

The driving "kicks" of the interferometer are imparted by laser pulses tuned to induce Raman transitions, a two-step process that takes advantage of a high-energy intermediate state: the atom absorbs photon of frequency ω_1 to reach level $|i\rangle$ and emits photon of frequency ω_2 to descend to state $|e\rangle$ (see Figure 3). The Doppler sensitivity is determined by the two transitions, each imparting momentum proportional to its respective driving ω, and the total can be approximated by $\Delta\omega_D \approx 2\vec{k} \cdot \vec{v}$.

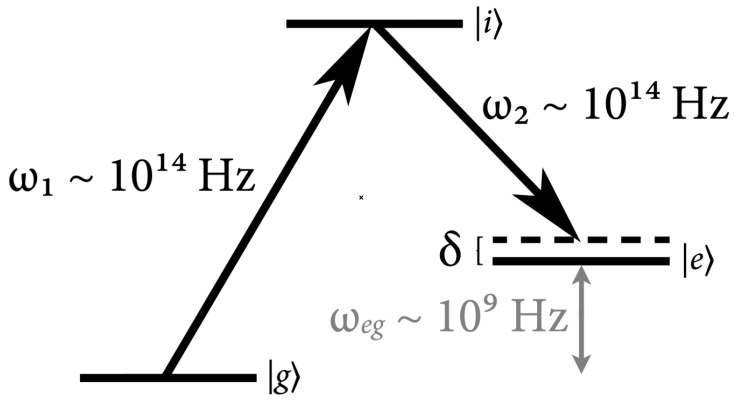

Figure 3

While ω_{eg} is small, ω_1 and ω_2 can be made very large to transfer high momentum transfer (about 10^4–10^5 times higher than with basic Rabi oscillation between $|e\rangle$ and $|g\rangle$). This is because the first pulse stimulates an absorption, and the second two emissions, so that $\Delta p \cong 2k_2$ to conserve momentum. This allows us to detect gravitational perturbations of $\sim 10^{-10}$ g, which effect phase perturbations of approximately 10^{-2}–10^{-1} radians (with visible light pulses driving the Raman transitions), which is an easily measurable change. Note that with microwaves ($\sim$1 GHz), the change is considerably smaller and not feasibly measurable.[4] The overall interferometer phase shift is given by $\vec{k} \cdot \delta\vec{x}(0) - 2\vec{k} \cdot \delta\vec{x}(T) + \vec{k} \cdot \delta\vec{x}(2T)$.

2.4 Impact of more realistic physics

Because laser sources do not have instant turn-on and turn-off, however, pulses do not have the ideal square wave shape. The effect on the cold atoms, then, is not quite what theoretical results following this assumption would predict. These differences are not extremely large, since the motion of the atoms during the brief turn-on and -off is not substantial (it takes about 100 μs), but they are still significant because of the atoms' small wavelength.

We want to understand the impact of more realistic laser drive on the entangling process used to set up the cold-atom interferometer, including finite pulse turn-on and frequency jitter.

3 Sequence of Hamiltonians

In order to gain a better understanding of the mechanisms behind the interferometers, we model the system with a sequence of Hamiltonians of increasing complexity. Starting from simple cases to gain intuitive insight into the behaviour of the atomic states, we add more and more considerations to the problem, making the model progressively more realistic and accurate, but at the same time, making analytic solving more difficult.

In the simplest case, we consider only the excitation of the atoms:

$$\widehat{H}_1 = \hbar\omega_g |g\rangle\langle g| + \hbar\omega_e |e\rangle\langle e|, \tag{1}$$

where $|g\rangle$ is the ground state, $|e\rangle$ is the excited state, and ω_g, ω_e are their respective characteristic frequencies. In this case, the atom has no external influences, and so the eigenstates are the ground and excited states over all time. In a proper chosen rotating frame, the wave function is then constant in time.

But once the external influence of the electromagnetic wave is explicit, the atom's state is no longer invariant through time:

$$\widehat{H}_2 = \widehat{H}_1 - \vec{d}\cdot\vec{E}\cos\omega t, \tag{2}$$

where $\vec{d}$ is the atomic electric dipole moment, and $\vec{E}, \omega$ are the driving electromagnetic wave amplitude and frequency, respectively.

This approximation holds when the wavelength of the electromagnetic pulse is much greater than the dimensions of the atomic beam. For optical frequencies and sufficiently fast atoms, however, we must also account for the particles' momenta:

first we modify the term for the electromagnetic wave,

$$\widetilde{H}_2 = \widehat{H}_1 - \vec{d} \cdot \vec{E} \cos(\vec{k} \cdot \vec{x} + \omega t), \tag{3}$$

and then we add an appropriate momentum term,

$$\widehat{H}_3 = \frac{\hat{p}^2}{2m} + \widetilde{H}_2, \tag{4}$$

where $\vec{k}$ is the wave vector of the driving electromagnetic wave, $\vec{x}$ is the position of the atom, and $\hat{p}$ is its momentum operator.

Now we consider the case of two detuned electromagnetic waves, whose system is described by a Hamiltonian with two terms for electromagnetic waves:

$$\begin{aligned}\widehat{H}_4 = \frac{\hat{p}^2}{2m} &+ \hbar\omega_g |g\rangle\langle g| + \hbar\omega_e |e\rangle\langle e| + \hbar\omega_i |i\rangle\langle i| \\ &- \vec{d} \cdot \Big(\vec{E}_1 \cos(\vec{k}_1 \cdot \vec{x} + \omega_1 t + \phi_1) + \vec{E}_2 \cos(\vec{k}_2 \cdot \vec{x} + \omega_2 t + \phi_2)\Big).\end{aligned} \tag{5}$$

With suitable assumptions, the above Hamiltonians can be solved analytically. We can therefore compare numerical results to those analytical solutions.

Taking into account non-instant laser turn-on and finite laser drive, we modify the electromagnetic wave terms to obtain

$$\begin{aligned}\widehat{H}_5 = \frac{\hat{p}^2}{2m} &+ \hbar\omega_g |g\rangle\langle g| + \hbar\omega_e |e\rangle\langle e| + \hbar\omega_i |i\rangle\langle i| \\ &- \vec{d} \cdot \Big(\vec{E}_1(t) \cos(\vec{k}_1 \cdot \vec{x} + \omega_1 t + \phi_1) + \vec{E}_2(t) \cos(\vec{k}_2 \cdot \vec{x} + \omega_2 t + \phi_2)\Big).\end{aligned} \tag{6}$$

Finally, a key effect still yet to be considered is the motion of the atoms in the gravitational field as the laser turns on and off. We therefore add a gravitational potential term, giving

$$\begin{aligned}\widehat{H}_6 = \frac{\hat{p}^2}{2m} &+ mgh + \hbar\omega_g |g\rangle\langle g| + \hbar\omega_e |e\rangle\langle e| + \hbar\omega_i |i\rangle\langle i| \\ &- \vec{d} \cdot \Big(\vec{E}_1(t) \cos(\vec{k}_1 \cdot \vec{x} + \omega_1 t + \phi_1) + \vec{E}_2(t) \cos(\vec{k}_2 \cdot \vec{x} + \omega_2 t + \phi_2)\Big).\end{aligned} \tag{7}$$

The treatment of this Hamiltonian, however, is outside of the scope of this report.

4 Results

Our goal is to solve the Schrödinger equation for these models without approximations, allowing us to study more realistic laser drive. We benchmark our numerical technique against existing solutions for special cases. In predicting the behaviour of the atoms, it is convenient to factor out the fast oscillation terms. This allows us to observe the system from a rotating frame of reference, so that the eigenfunctions of $\widehat{H}_1$ are constant in time. Upon adding the external influence of an electromagnetic wave ($\widehat{H}_2$), however, the system evolves, with a non-trivial wave function evolution (see Figure 4).

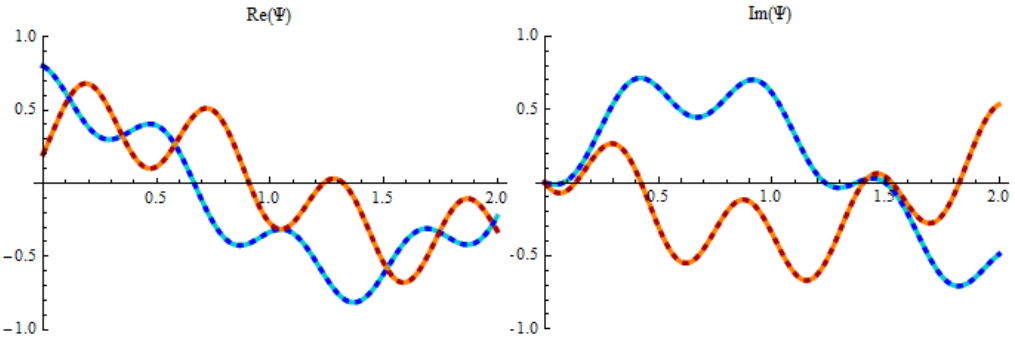

Figure 4: Time evolution of the real (left) and imaginary (right) parts of the excited (blue) and ground state (orange) wave functions. Dotted lines are analytical results from [1].

We now consider the more complex case of counter-propagating waves – that is, two laser pulses of different frequency travelling in opposite directions. The system becomes considerably more complex, now being able to undergo Raman transitions, so that the system is effectively three-level. It is possible, however, to simplify the model in cases where the energy of the lasers is sufficiently high, so that the system again becomes two-level ($\widehat{H}_4$; see Figure 5).

Our numerical results are in close agreement with analytical solutions, which verify the validity of our simulations. Our models, then, offer a numerical alternative to find solutions to the Schrödinger equation of more complex systems (such as those with realistic laser drives – e.g., $\vec{E}(t)$, $\vec{k}(t)$), where no analytic solutions have yet been found. Let us now introduce a basic consideration: finite laser wavetrain with gradual turn-on and turn-off. We model this by defining $E(t)$ of the form

$$E(t) = \left(\frac{1}{\pi}\arctan \alpha t + \frac{1}{2}\right)\left(\frac{1}{\pi}\arctan(-\alpha t + \alpha\beta) + \frac{1}{2}\right).$$

Because the characteristic laser frequencies are typically much higher than the

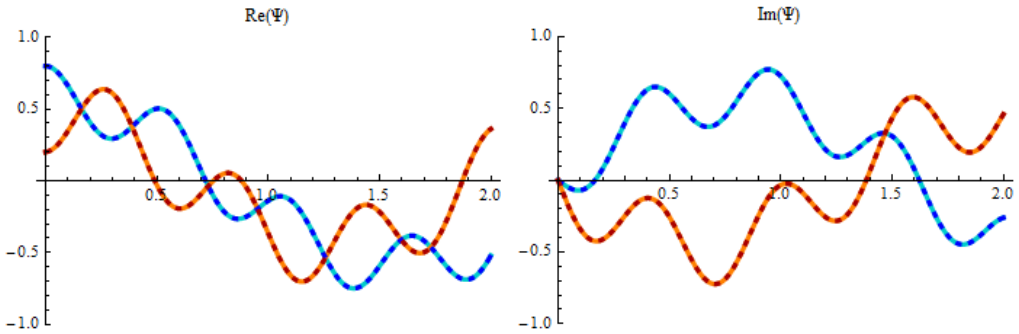

Figure 5: The evolution of the excited and ground state wave functions show the required Rabi oscillations for interferometry.[1]

reciprocals of the pulse lengths, however, the number of oscillations is extremely high, making numerical calculations quite difficult for slower machines. Had we access to more powerful machines, the full power of the numerical solution could be realised. As such, therefore, we have chosen values such that the relative mag-

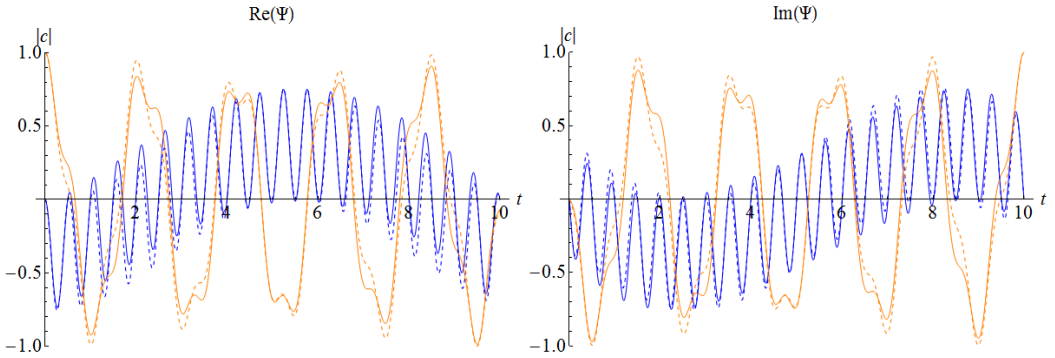

Figure 6: Orange and blue lines denote the complex coefficients of the ground and excited states of the wave function. Darker dotted lines are the time evolution under an infinite wave train and solid lines are time evolution under a finite pulse.

nitudes obey their real physical relation – i.e.,

$$\omega_e, \omega_g > \omega_{eg} > \alpha > \frac{1}{\beta},$$

where each inequality manifests a difference of at least an order of magnitude in the simulation paramaters. Accordingly, we find that the change due to this consideration is significant (see Figure 6). Further confirmation for the reliability of these models could come from investigating limiting cases of turn-on time

to approach the infinite wave train ideal. With better resources, moreover, future work can solve the problem with more physically realistic parameters, which would give the desired numerical wave function solutions to this complex problem, which might otherwise be very difficult to solve analytically. Additionally, the gravitational potential, while difficult to account for analytically, can also be investigated numerically ($\widehat{H}_6$).

Acknowledgements

Special thanks to Steve Libby and Vijay Sonnad for insightful discussions and patient mentoring throughout this project.

This work was performed under the auspices of the US Department of Energy by Lawrence Livermore National Laboratory under Contract DE-AC52-07NA27344. This work was supported in part by the U.S. Department of Energy, Office of Science, Office of Workforce Development for Teachers and Scientists (WDTS) under the Science Undergraduate Laboratory Internships Program (SULI), and partially supported by DHS/DNDO contract CFP11-100-RTA-06-FP007, HSHQDC-11-X-00550.

References

[1] B. Young, M. Kasevich, and S. Chu. "Precision Atom Interferometry with Light Pulses", in *Atom Interferometry*, ed. Paul Berman, Academic Press: 1997.

[2] O. Carnal and J. Mlynek. "Young's double-slit experiment with atoms: A simple atom interferometer", *Phys. Rev. Lett.* **66** (1991), 2689.

[3] M. de Angelis, et al. "Precision gravimetry with atomic sensor", *Meas. Sci. Technol.* **20,** 022001 (2009).

[4] S. B. Libby, et al. "Feasibility Study of a Passive, Standoff Detector of High Density Masses with a Gravity Gradiometer Based on Atom Interferometry", LLNL-TR-465878, 2011.

[5] M. Kasevich and S. Chu. "Atomic interferometry using stimulated Raman transition", *Phys. Rev. Lett.* **67** (1991), 181–184.

[6] A. Peters, K. Y. Chung and S. Chu. "High-precision gravity measurements using atom interferometry", *Metrologia*, 2001, **38,** 25–61.